# E-cadherin is required for intestinal morphogenesis in the mouse

Benjamin J. Bondow, Mary L. Faber, Kevin J. Wojta, Emily M. Walker, Michele A. Battle*

Department of Cell Biology, Neurobiology and Anatomy, Medical College of Wisconsin, 8701 Watertown Plank Road, Milwaukee, WI 53226, USA

## ARTICLE INFO

## ABSTRACT

E-cadherin, the primary epithelial adherens junction protein, has been implicated as playing a critical role in nucleating formation of adherens junctions, tight junctions, and desmosomes. In addition to its role in maintaining structural tissue integrity, E-cadherin has also been suggested as an important modulator of cell signaling via interactions with its cytoplasmic binding partners, catenins, as well as with growth factor receptors. Therefore, we proposed that loss of E-cadherin from the developing mouse intestinal epithelium would disrupt intestinal epithelial morphogenesis and function. To test this hypothesis, we used a conditional knockout approach to eliminate E-cadherin specifically in the intestinal epithelium during embryonic development. We found that E-cadherin conditional knockout mice failed to survive, dying within the first 24 hours of birth. Examination of intestinal architecture at E18.5 demonstrated severe disruption to intestinal morphogenesis in animals lacking E-cadherin in the epithelium of the small intestine. We observed changes in epithelial cell shape as well as in the morphology of villi. Although junctional complexes were evident, junctions were abnormal, and barrier function was compromised in E-cadherin mutant intestine. We also identified changes in the epithelial cell populations present in E-cadherin conditional knockout animals. The number of proliferating cells was increased, whereas the number of enterocytes was decreased. Although Wnt/β-catenin target mRNAs were more abundant in mutants compared with controls, the amount of nuclear activated β-catenin protein was dramatically lower in mutants compared with controls. In summary, our data demonstrate that E-cadherin is essential for intestinal epithelial morphogenesis and homeostasis during embryonic development.

© 2012 Elsevier Inc. All rights reserved.

## Introduction

As proper epithelial morphogenesis is essential for organ function, defining the roles that specific cell junction and adhesion molecules play in driving formation and maintenance of epithelial structure is necessary. Several studies of E-cadherin revealed an important role for this cell adhesion molecule in epithelial organization and maintenance (Perez-Moreno et al., 2003; Schneeberger and Lynch, 2004; Van Roy and Berx, 2008). For example, Madin–Darby canine kidney (MDCK) cells incubated with anti-E-cadherin antibodies failed to assemble not only adherens junctions but also tight junctions and desmosomes implicating E-cadherin as required for junctional complex formation (Gumbiner et al., 1988; Troxell et al., 2000). Studies of E-cadherin in vivo have been less clear in defining an essential role for E-cadherin in junctional complex assembly. Global knockout suggested that E-cadherin was required because the trophectoderm epithelium failed to form in its absence (Larue et al., 1994). Conditional ablation of E-cadherin from mammary

epithelium, epidermis, thyroid follicular epithelium, and hepatic epithelium, however, did not result in tight junction or desmosome loss although epidermal deletion caused increased tight junction permeability and neonatal lethality because of a non-functional skin water barrier (Boussadia et al., 2002; Young et al., 2003; Tinkle et al., 2004; Tunggal et al., 2005; Battle et al., 2006; Cali et al., 2007). Studies looking at E-cadherin in the intestinal epithelium demonstrated a key role for E-cadherin in the maintenance of normal intestinal epithelial homeostasis (Hermiston and Gordon, 1995a, 1995b; Hermiston et al., 1996). Expression of a dominant-negative N-cadherin protein (NCADΔ) in villus enterocytes caused loss of endogenous E-cadherin protein resulting in cell adhesion and shape defects. Barrier function was also defective in NCADΔ-expressing enterocytes. Crypt cells that lacked NCADΔ protein and therefore maintained endogenous E-cadherin protein showed increased proliferation, which likely compensated for defective enterocytes on the villus (Hermiston and Gordon, 1995a). In contrast, over-expression of E-cadherin in mice resulted in slower cellular migration from crypt to villus, decreased proliferation, and increased apoptosis (Hermiston et al., 1996). Recently, Schneider et al. (2010) used tamoxifen-inducible Villin-Cre to remove E-cadherin from the adult mouse intestinal epithelium. Animals lacking E-cadherin developed

* Corresponding author. Fax: +1 414 955 6517.
E-mail address: mbattle@mcw.edu (M.A. Battle).

hemorrhagic diarrhea requiring euthanasia. Epithelial architecture was abnormal with cells shedding into the lumen. There were changes in maturation and positioning of secretory lineages (goblet and Paneth cells). The proliferative zone was markedly expanded, and increased numbers of apoptotic cells were present. Migration of cells along the villus was also enhanced. Moreover, in contrast to deletion in other organ systems in which junctional complex assembly was unaffected by elimination of E-cadherin, loss of E-cadherin from the adult intestinal epithelium resulted in loss of both adherens junctions and desmosomes whereas tight junctions were unaffected (Schneider et al., 2010). The functionality of tight junctions, however, was not assessed.

Because E-cadherin has been implicated as playing critical roles in epithelial cell adhesion and signal transduction and because modulation of its expression in the adult small intestine caused epithelial defects, we proposed that loss of E-cadherin from the developing mouse intestinal epithelium would result in severe disruption of intestinal epithelial morphogenesis and homeostasis. Therefore, to assess the role that E-cadherin plays in intestinal development, we employed a conditional knockout approach using a non-inducible Villin-Cre, which directs robust recombination in the intestinal epithelium during development (Madison et al., 2002). We found that neonates lacking intestinal E-cadherin died shortly after birth. Villus structure and cell shape were both abnormal, and barrier function was compromised. We observed a decrease in the total number of epithelial cells present in mutant tissue. Of the specific differentiated cell types, enterocytes were lost whereas secretory populations were relatively stable. Proliferation was increased in animals with an E-cadherin deficient intestinal epithelium, and apoptosis was unchanged. Finally, β-catenin levels were decreased in mutant intestine compared with control. Paradoxically, we detected increased mRNA abundance of several β-catenin transcriptional targets in mutant epithelium compared with control epithelium. Based on these data, we conclude that intestinal E-cadherin expression is required for formation and maintenance of a functional intestinal epithelium in mice.

## Materials and methods

### Animals

Derivation of $Cdh1^{loxP}$ ($Cdh1^{tm2Kem}$) and Villin-Cre (Tg(Vil-cre)997Gum) mice has been previously described (Boussadia et al., 2002; Madison et al., 2002). Embryonic mice were generated by timed matings considering noon on the day of a vaginal plug as E0.5. Genotypes were determined by PCR analysis of ear punch DNA following a standard protocol. PCR primers used were: $Cdh1^{loxP}$, gtgacaggaaaggcatatcagcaacaagat, gtgagctggtacccatggaggacactga; Villin-Cre caagcctggctcgacggcc, cgcgaacatcttcaggttct. For proliferation studies, 200 μg 5-ethynyl-2'deoxyuridine (EdU) was administered by intraperitoneal injection three hours prior to euthanizing animals. The Medical College of Wisconsin's Animal Care Committee approved all animal procedures used in this study.

### Histochemistry, immunohistochemistry, and immunofluorescence

Tissue harvested from the midpoint of E18.5 small intestine was fixed in zinc formalin or 4% paraformaldehyde. Hematoxylin and eosin staining and alcian blue staining were performed according to standard procedures (Bancroft and Gamble, 2007). The Vector Red Phosphatase Substrate Kit (Vector Labs, Burlingame, CA) was used to detect alkaline phosphatase activity. For immunohistochemistry, antibodies were applied to tissue after citric acid antigen retrieval. To visualize staining, R.T.U. Vectastain Elite ABC reagent (Vector Labs, Burlingame, CA) and a Metal Enhanced DAB substrate kit (Thermo Scientific, Rockford, IL) were used. For immunofluorescence, fresh frozen sections were fixed with 3% paraformaldehyde prior to antibody staining. DAPI (Invitrogen, Carlsbad, CA; 1:5000) was used to visualize nuclei. EdU staining was performed using the Click-it Edu Alexa-Fluor 594 kit (Invitrogen, Carlsbad, CA). See Supplemental Table 1 for antibody details.

### Electron microscopy

Embryonic (E18.5) small intestine was dissected into 2.5% glutaraldehyde in 0.1 M cacodylate buffer and embedded in EPON 812 epoxy resin. Sections (60 nm) were contrasted with uranyl acetate and lead citrate. For tracer experiments, embryonic mouse gut was dissected into sodium cacodylate buffer pH 7.4 and fixed in 2% glutaraldehyde containing either Lanthanum nitrate or Ruthenium red tracers (Lewis and Knight, 1992). Sections were examined using a Hitachi 600 transmission electron microscope.

### Oligonucleotide array analysis

Total RNA (300 ng) isolated from three independent control and experimental E18.5 small intestines was used to prepare oligonucleotide array probes following the protocol described in the GeneChip Whole Transcript Sense Target Labeling Assay manual (Affymetrix, Santa Clara, CA). We hybridized a total of six Mouse Gene 1.0 ST arrays (Affymetrix, Santa Clara, CA), three for control samples and three for experimental samples, with fragmented, biotinylated ssDNA probes. Images were acquired using a GeneChip Scanner 3000 (Affymetrix, Santa Clara, CA). GeneChip Operating Software (GCOS) and NetAffx from Affymetrix, dChip 2010 software (Li and Wong, 2001), and Ingenuity Pathway Analysis software were used in combination to analyze the data. Log-transformed gene expression values were determined using dChip 2010. We selected a fold-change cutoff of $+/-2.0$ fold, $p \le 0.05$. Differentially expressed transcript identifiers annotated using NetAffx are listed in Supplemental Table 2. The set of differentially expressed genes was analyzed by IPA for biological function analysis according to the method outlined in the Ingenuity 9.0 manual.

### Epithelial cell isolation

Small intestine harvested from control and E-cadherin cKO E18.5 embryos was cut along its longitudinal axis and incubated in cell dissociation buffer (BD Biosciences, San Jose, CA) for 6 h at 4 °C with gentle agitation to release epithelial cells (Madison et al., 2005; Li et al., 2007).

### Quantitative reverse transcription polymerase chain reaction (qRT-PCR)

DNase treated total RNA isolated from epithelial cells of three independent control and E-cadherin mutant E18.5 intestines was used to generate cDNA with the Superscript VILO cDNA synthesis kit (Invitrogen, Carlsbad, CA). qRT-PCR was performed using TaqMan assays and TaqMan Gene Expression Master Mix (Applied Biosystems, Carlsbad, CA). TaqMan assays utilized are listed in Supplemental Table 3. Data were analyzed using DataAssist software (Applied Biosystems, Carlsbad, CA). Gapdh was used for normalization. Each gene was assayed in at least two independent experiments. Error bars represent standard error of the mean (SEM).

## Immunoblotting

Protein was extracted from tissue or isolated epithelial cells of control and E-cadherin mutant E18.5 small intestines. For whole cell extracts, cell pellets were lysed in buffer containing 0.5% NP-40, 50 mM Tris–HCl, pH 8.0, 10% glycerol, 0.1 mM EDTA, 250 mM NaCl, and HALT[TM] Protease Inhibitor cocktail without EDTA (Thermo Scientific, Rockford, IL). For nuclear extracts, cells were lysed using the NE-PER Nuclear and Cytoplasmic Extraction Reagents (Thermo Scientific, Rockford, IL), HALT[TM] Protease Inhibitor cocktail without EDTA (Thermo Scientific, Rockford, IL), and HALT[TM] Phosphatase Inhibitor cocktail (Thermo Scientific, Rockford, IL). Proteins (5 μg whole cell extract or 2.5 μg nuclear extract) separated using Nu-PAGE Bis-Tris 4–12% gradient gels (Invitrogen, Carlsbad, CA) were transferred to Immun-Blot poly-vinylidene difluoride (PVDF) membrane (Bio-Rad, Hercules, CA) by wet transfer using NuPAGE transfer buffer (Invitrogen, Carlsbad, CA) with 10% methanol and 0.01% SDS. Antibodies utilized are listed in Supplemental Table 1.

## Results

### Deletion of E-cadherin from the intestinal epithelium results in neonatal lethality

We employed a conditional knockout approach to eliminate E-cadherin specifically in the intestinal epithelium during embryonic development. Upon genotyping 193 weanlings, we identified only one animal with the mutant Cdh1[loxP/loxP] Villin-Cre genotype (Table 1), and this animal showed normal levels of E-cadherin likely reflecting inefficiency of Cre recombinase (data not shown). Based on these data, we conclude that E-cadherin conditional knockout (cKO) mice fail to survive. Therefore, we sought to determine the age at which loss of E-cadherin results in lethality. Observation of newborn pups revealed a subset that were lethargic with distended, dark abdomens within 6 to 12 h of birth (Fig. 1A). A notably smaller milk spot was also observed. Genotyping of these pups demonstrated their genotype to be Cdh1[loxP/loxP] Villin-Cre (E-cadherin cKO). Examination of the gross anatomy of the dissected gastrointestinal tract revealed that mutant pups had a dilated small intestine lacking normal appearing yellow chyme and instead containing dark fluid (Fig. 1B). Moreover, small intestine length differed significantly between controls and E-cadherin mutants (Fig. 1C). Analysis of hematoxylin-eosin stained intestinal tissue sections harvested from control and E-cadherin cKO embryos at E18.5 showed that loss of E-cadherin severely disrupted intestinal morphogenesis (Fig. 1D). Villi of mutant intestine were either absent or severely blunted and misshapen, and mutant intestinal epithelial cells were rounded instead of the typical columnar morphology (Fig. 1D). We verified loss of E-cadherin protein in the small intestine of E-cadherin cKOs by immunoblot and immunohistochemistry (Fig. 1E and 1F). Although Villin-Cre becomes active in the intestine by E14.5 (Madison et al., 2002), we found that robust loss of E-cadherin protein was not evident until E17.5–E18.5.

**Table 1**
E-cadherin [loxP/loxP]Villin-Cre mice fail to survive to weaning age of 3 weeks.

| Genotype | Number of weanlings |
| --- | --- |
| E-cadherin [loxP/+] | 51 |
| E-cadherin [loxP/loxP] | 77 |
| E-cadherin [loxP/+] Villin-Cre | 64 |
| E-cadherin [loxP/loxP]Villin-Cre | 1 |

Therefore, we chose to focus on the phenotype at E18.5 when loss of E-cadherin protein was maximal.

### Barrier function is disrupted in E-cadherin cKO small intestine

Although studies of E-cadherin in multiple organ systems failed to demonstrate an essential role for E-cadherin in junctional complex assembly (Boussadia et al., 2002; Young et al., 2003; Tinkle et al., 2004; Tunggal et al., 2005; Battle et al., 2006; Cali et al., 2007), elimination of E-cadherin in the adult intestinal epithelium resulted in loss of adherens junctions and desmosomes (Schneider et al., 2010). Therefore, we determined the status of cell-cell junctions in E18.5 control and E-cadherin mutant small intestine. In control tissue, adjacent cells were tightly associated as a simple columnar epithelium (Fig. 2A, upper left). Mutant epithelial cells, however, appeared loosely connected and had a rounded morphology (Fig. 2A, upper right). Microvillus morphology appeared unchanged between controls and mutants. Higher magnification inspection of cell-cell junctions in control tissue showed extensive, well-developed junctional complexes (Fig. 2A, lower left). Despite the abnormal appearance of the intestinal epithelium, we observed junctional complexes throughout the E-cadherin mutant tissue although qualitatively these junctions were abbreviated compared with those of control tissue (Fig. 2A, lower right). To evaluate junction integrity, we used tracer molecules in combination with transmission electron microscopy. As expected, junctions present in control intestinal epithelium prevented passage of tracers into the intercellular space (Fig. 2B, left). Tracer presence on the lateral cell membrane was detected in only 4 of 100 junctions observed in control tissue. In contrast, E-cadherin cKO intestinal epithelium failed to block paracellular tracer passage (Fig. 2B, right). We detected tracer penetration at 88 of 100 junctions observed in mutant tissue. Based on these data, we conclude that although tight junctions are present in E-cadherin mutant intestinal epithelium, these junctions are abnormal and that barrier function is compromised.

### Loss of E-cadherin in the intestinal epithelium results in widespread changes in gene expression

In addition to promoting cell-cell adhesion, cadherin molecules have been implicated as important modulators of cell signaling via interactions with cytoplasmic binding partners such as catenins (McCrea et al., 2009; Cavallaro and Dejana, 2011). Moreover, cadherin molecules have been shown to modulate signaling and gene expression through interactions with growth factor receptors including the FGF receptor and the EGF receptor (McCrea et al., 2009; Cavallaro and Dejana, 2011). Therefore, we performed Affymetrix oligonucleotide array analysis to identify genes with altered expression in E-cadherin mutant intestinal tissue compared with control tissue. Using dChip, we compared the small intestinal gene expression profiles of three control and three E-cadherin cKOs at E18.5. We identified 371 genes with expression increased $\geq 2.0$ fold ($p \leq 0.05$) and 522 genes with expression decreased $\geq 2.0$ fold ($p \leq 0.05$) (Supplemental Table 2). We utilized Ingenuity Pathway Analysis (IPA) software to categorize these genes and examined the top five affected biological functions. We found cellular movement, cellular growth and proliferation, cell-to-cell signaling, cell morphology, and cellular development as the top five biological functions identified from the data set of genes with increased expression in E-cadherin mutant intestine compared with control intestine (Fig. 3). We found lipid metabolism, small molecule biochemistry, vitamin and mineral metabolism, amino acid metabolism, and cell signaling as the top five biological functions identified from the data set
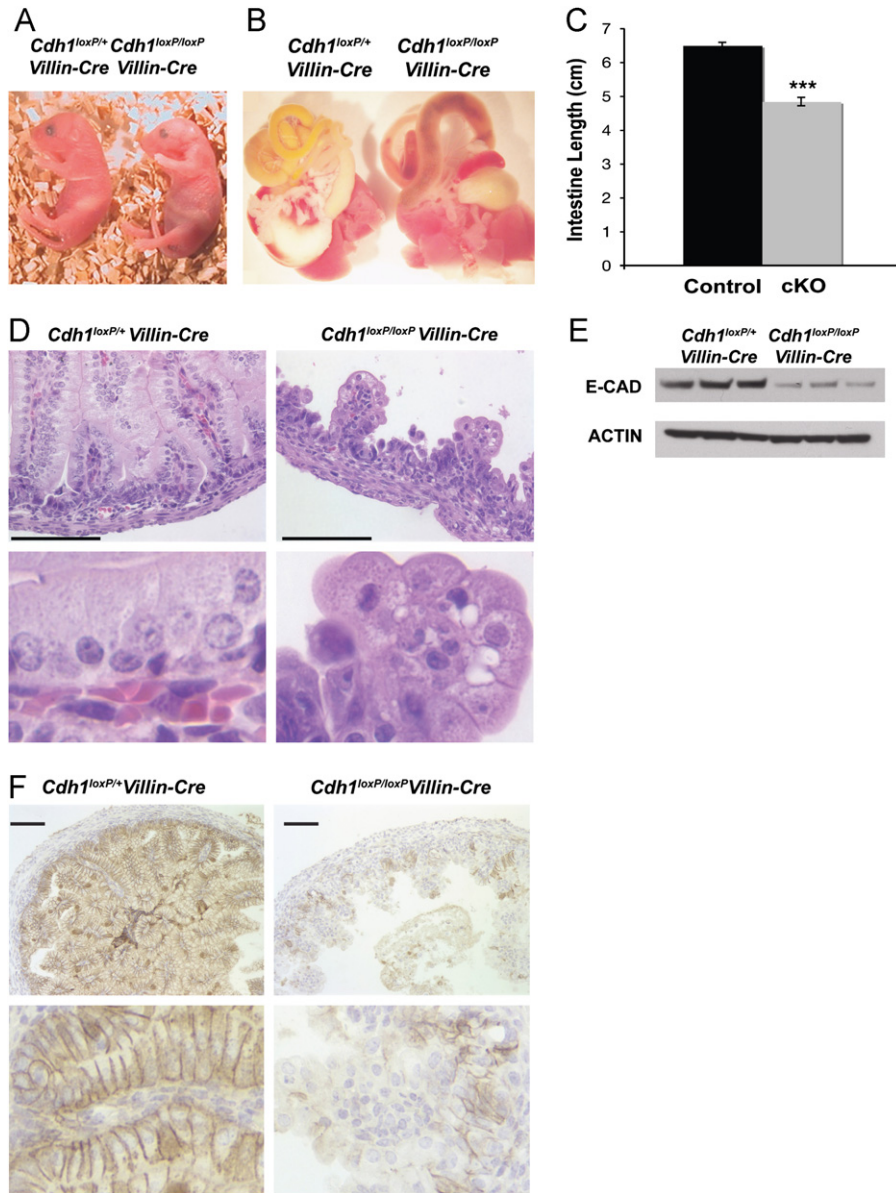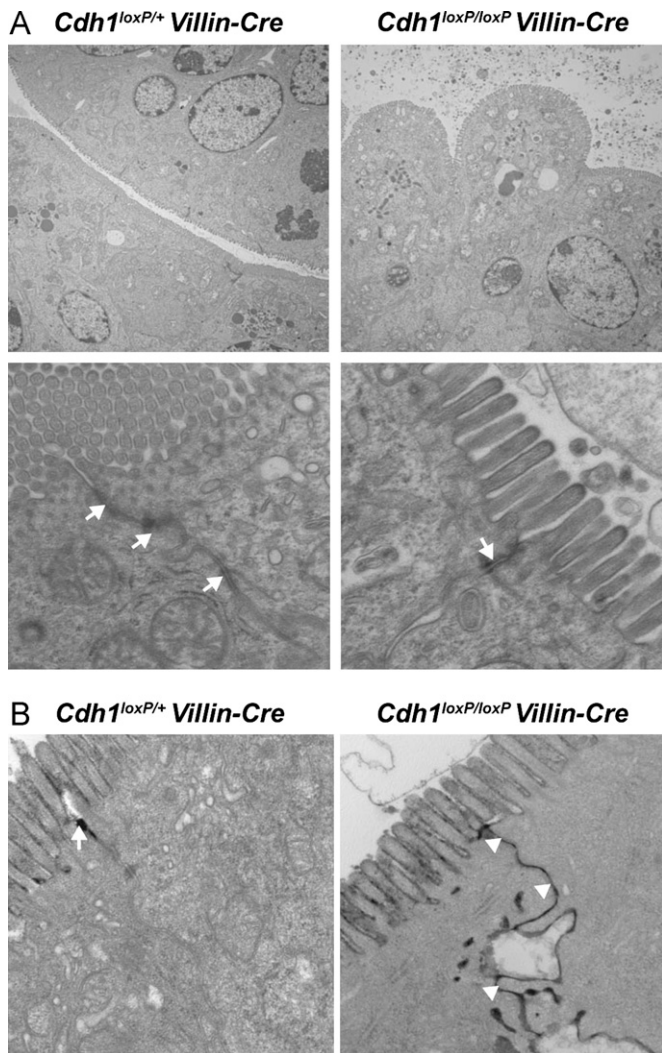
**Fig. 1.** Deletion of E-cadherin in the small intestinal epithelium results in neonatal lethality. (A) Image shows control *Cdh1*^loxP/+ *Villin-Cre* (left) and experimental *Cdh1*^loxP/loxP *Villin-Cre* (right, cKO) neonatal pups. Overall size of the pups was similar. The milk spot was apparent in the control pup, whereas it was not distinct in the cKO pup. Moreover, the mutant pup had a distended abdomen, which appeared dark in color, making the *E-cadherin* cKO pups readily distinguishable from control litter mates after birth. (B) Image shows gastrointestinal tracts harvested from neonatal control *Cdh1*^loxP/+ *Villin-Cre* (left) and experimental *Cdh1*^loxP/loxP *Villin-Cre* (right, cKO) pups. The control intestine contained normal yellow appearing chyme, whereas the mutant intestine was dilated and contained a dark fluid. (C) Small intestine length (cm) of control (n=55) and *Cdh1*^loxP/loxP *Villin-Cre* cKO (n=42) E18.5 embryos was measured. Mutant small intestines (gray bar) were shorter than control small intestines (black bar). Error bars show SEM. A two-sample Student t test was used to determine p-value (***$p \leq 0.001$). (D) Hematoxylin and eosin stained small intestine from control (left) and *Cdh1*^loxP/loxP *Villin-Cre* cKO (right) E18.5 mice demonstrated severe disruption of the intestinal epithelium in cKO mice compared with controls. Villi were severely blunted or absent in cKO mice. Cell shape was altered from the normal columnar morphology to a rounded morphology. Lower panels represent higher magnification images taken from a region of the original image. Scale bar =100 μm. (E) Immunoblot analysis of E18.5 whole cell extracts demonstrated a decreased amount of E-cadherin protein in intestine of *Cdh1*^loxP/loxP *Villin-Cre* cKO embryos compared with controls. β-ACTIN was used as the loading control. (F) E-cadherin protein (brown membrane staining) was detected ubiquitously throughout the epithelium of control E18.5 small intestine using immunohistochemistry. E-cadherin protein, however, was absent from the majority of the epithelium in E18.5 mutant small intestine. Lower panels represent higher magnification images taken from a region of the original image. Scale bar=100 μm.

of genes with decreased expression in E-cadherin mutant intestine compared with control intestine (Fig. 3).

*Expression of claudins is altered in E-cadherin mutant intestine*

Because we found that tight junction integrity was compromised in E-cadherin mutant intestine, we examined our gene array data to identify changes in expression of tight junction components and found several claudin transcripts as aberrantly expressed in mutant intestine. *Claudin 1* (*Cldn1*) expression was decreased −3.9 fold in mutants compared with controls; levels of both *Claudin 3* (*Cldn3*) and *Claudin 4* (*Cldn4*) were increased in mutants compared with controls, +2.3 and +8.5 fold, respectively. qRT-PCR confirmed *Cldn1* transcript to be decreased (−16.4) and *Cldn3* and *Cldn4* transcripts to be increased (+2.4 and +14.2, respectively) (Fig. 4A). Both CLDN1 and CLDN4

## A

**Cdh1^{loxP/+} Villin-Cre**          **Cdh1^{loxP/loxP} Villin-Cre**



## B

**Cdh1^{loxP/+} Villin-Cre**          **Cdh1^{loxP/loxP} Villin-Cre**



**Fig. 2.** The epithelial barrier is disrupted in small intestine lacking E-cadherin. (A) Control and Cdh1^{loxP/loxP} Villin-Cre cKO intestinal tissue harvested at E18.5 was analyzed using transmission electron microscopy (TEM). Top panel shows images at low magnification demonstrating the altered cellular shape observed in the intestinal epithelium of *E-cadherin* cKO embryos. Instead of containing tightly packed, columnar enterocytes as in control tissue (left), mutant tissue contained loosely associated, rounded epithelial cells (right). Lower panel demonstrates that both control and *E-cadherin* cKO tissue contained junctional complexes (white arrows). Such complexes, however, were smaller and less elaborated in mutant tissue compared with control tissue. These complexes were observed in the pits between the rounded mutant cells. (B) To assess the integrity of the junctions present in mutant tissue, we incubated control and mutant tissue with tracer molecules during fixation and then processed these for TEM. Because the tracer molecules used cannot penetrate functional tight junctions, we observed punctate black staining at the apical surface between two juxtaposed control cells (white arrow). In contrast, we observed that the tracer molecule penetrated between mutant cells. Abundant black staining was evident along the lateral membrane of two juxtaposed mutant cells (white arrow heads).

protein levels were also changed (Fig. 4B); CLDN3 protein levels, however, were not found to be consistently increased in mutants compared with controls at E18.5 (Fig. 4B).

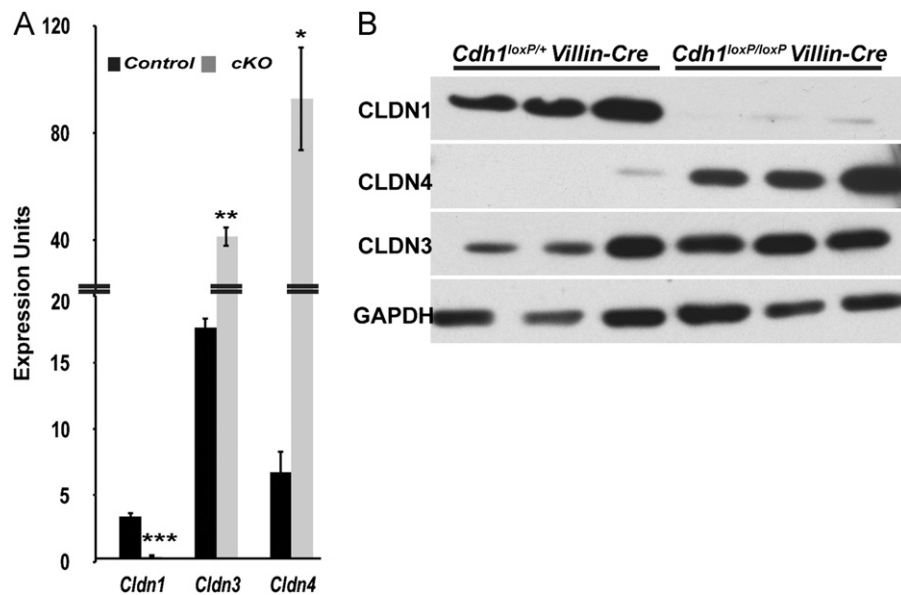### E-cadherin cKO intestinal epithelium contains increased proliferative cells compared with control epithelium

The finding that proliferation was one of the top five biological functions predicted by IPA software to increase in E-cadherin deficient intestine compared with control intestine led us to investigate in more detail proliferation in the absence of E-cadherin. Several transcripts involved in proliferation were identified by IPA as increased in E-cadherin mutants compared with controls including *CD44 antigen* (Cd44), *Cyclin-dependent kinase 6* (Cdk6), *Early growth response 1* (Egr1), and *Myelocytomatosis oncogene* (Myc). We performed qRT-PCR using RNA harvested from isolated intestinal epithelial cells and confirmed *Cd44*, *Cdk6*, *Egr1*, and *Myc* transcripts as significantly more abundant in E-cadherin mutant intestinal epithelium compared with control epithelium (Fig. 5A). In addition, although not identified by array analysis, we examined by qRT-PCR the expression of two additional characteristic cell proliferation markers, *Cyclin D1* (Ccnd1), which is the cyclin binding partner of CDK6 (Sherr, 1995), and *SRY-box containing gene 9* (Sox9), which marks the proliferative intervillus region of the small intestine (Bastide et al., 2007; Spence et al., 2011). We found both transcripts to be more abundant in E-cadherin deficient intestinal epithelium compared with control epithelium (Fig. 5A). In addition to containing increased *Myc* transcript, E-cadherin mutant intestine contained a greater abundance of MYC protein compared with control tissue (Fig. 5B). Increases in gene products involved in cellular proliferation in the intestinal epithelium of *E-cadherin* cKOs could represent single cells expressing these genes at higher levels or an increase in the total number of cells expressing these markers. Immunohistochemical staining for CD44 and SOX9 demonstrated increased staining in the intestinal epithelium of *E-cadherin* cKOs compared with that of controls (Fig. 5C) suggesting that these transcripts were more abundant because there are more proliferative cells in E-cadherin deficient intestine compared with control intestine. Therefore, to quantify proliferation in E18.5 control and E-cadherin mutant intestinal epithelium, we measured incorporation of 5-ethynyl-2'deoxyuridine (EdU) after a three hour pulse. The disorganized epithelial structure of the mutant intestine made it difficult to distinguish between proliferative cells residing in the epithelium and proliferative cells residing in the underlying connective tissue and muscle layers. Therefore, we stained tissue sections for EdU incorporation (proliferative cells), expression of laminin (a connective tissue marker), and DAPI (nuclear stain) (Fig. 6A). We counted DAPI+, LAM- cells to determine the total number of epithelial cells per field and EdU+,DAPI+, LAM- to determine the subset of proliferating epithelial cells per field ($n=53$ fields from 9 control animals and $n=62$ fields from 6 mutant animals). We found that mutant tissue contained roughly half the number of epithelial cells compared with control tissue (Figs. 6B, $215 \pm 8$ average epithelial cells per control field vs. $109 \pm 5$ average epithelial cells per mutant field, $p < 0.001$). Although there were fewer total epithelial cells in mutant tissue, proliferating cells were more abundant in mutants compared with controls. We observed a 20% increase in the number of proliferative cells in mutant epithelium compared with control epithelium (Figs. 6B, $37 \pm 2$ average EdU+ epithelial cells per control field vs. $44 \pm 3$ average EdU+ epithelial cells per mutant field, $p=0.054$).

Previous studies of E-cadherin function in the mouse intestine demonstrated changes in epithelial apoptotic cell death when E-cadherin levels were modulated (Hermiston et al., 1996; Schneider et al., 2010). The presence of cellular debris sloughed into the intestinal lumen of our mutants as well as our finding that there were fewer epithelial cells present in mutants compared with controls indicated that apoptosis was possibly changed in embryonic small intestine lacking E-cadherin. Therefore, we stained for apoptotic cells in intestinal tissue lacking E-cadherin using an antibody against active caspase 3. We failed to detect a change in apoptosis in the adherent epithelial cell population in intestinal tissue of *E-cadherin* cKO embryos compared with controls (Fig. 6C). We did, however, observe apoptotic
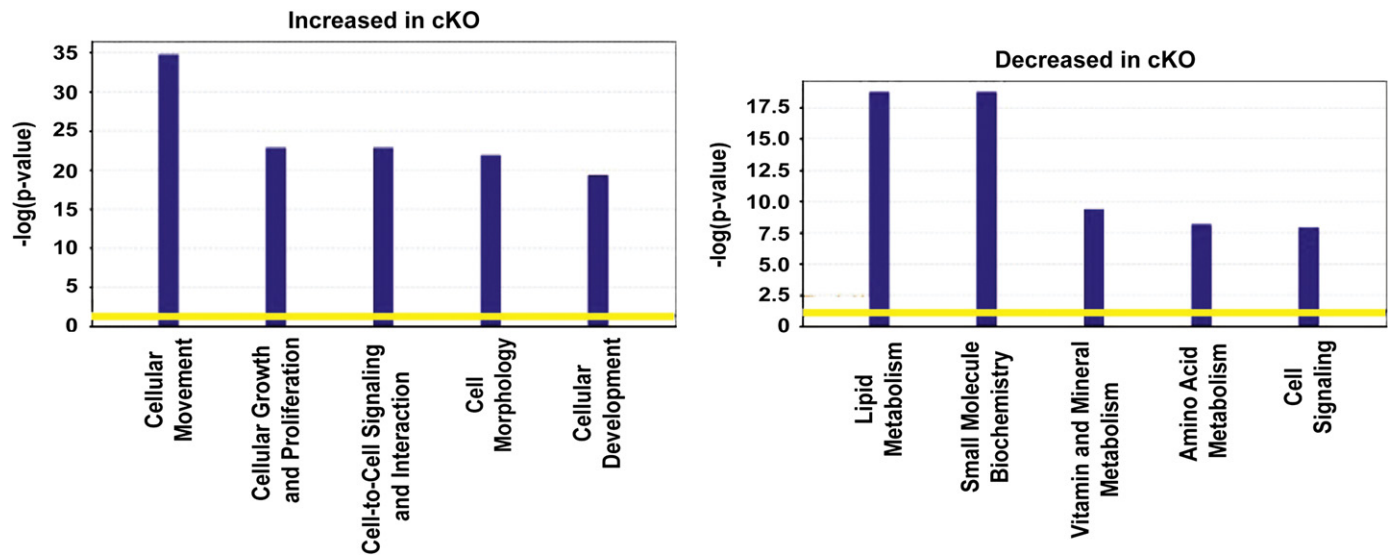
**Fig. 3.** Loss of E-cadherin in the small intestine resulted in changes in the gene expression profile of $Cdh1^{loxP/loxP}$ Villin-Cre cKO mice compared with controls. Ingenuity Pathway Analysis (IPA) software was used to analyze oligonucleotide array data collected from small intestinal RNA isolated from three independent control and three independent E-cadherin cKO embryos at E18.5. Signal values were computed using dChip 2010 software, and a data set containing those genes with expression changes $\geq 2.0$ ($p \leq 0.05$) between control and mutant tissue were inputed into IPA software. Of the 904 genes annotated by IPA software, 728 were associated with biological functions in Ingenuity's Knowledge Base and were therefore eligible for biological function analysis. Such analysis identified the biological functions that were most significant to the data set. A right-tailed Fisher's exact test was used to calculate a $p$-value determining the probability that each biological function assigned to that data set is due to chance alone. The $y$-axis displays significance as -log($p$-value). The yellow threshold line denotes $p=0.05$. The identified biological functions are listed on the $x$-axis. Left graph shows those functions most significantly associated with the set of genes with increased expression in mutant small intestine compared with control; right graph shows those functions most significantly associated with the set of genes with decreased expression in mutant small intestine compared with control.



**Fig. 4.** Claudin mRNA and protein levels are altered in $Cdh1^{loxP/loxP}$ Villin-Cre cKO small intestine compared with control tissue. (A) Levels of Claudin transcripts present in the intestinal epithelium of E18.5 control ($n=3$) and E-cadherin cKOs ($n=3$) were determined using qRT-PCR. Cldn1 was decreased, whereas Cldn3 and Cldn4 were increased. Gapdh was used for normalization. Error bars show SEM. A two-sample Student t test was used to determine $p$-value: $^*p \leq 0.05$, $^{**}p \leq 0.01$, $^{***}p \leq 0.001$ (B) Immunoblot analysis of E18.5 whole cell extracts demonstrated a decreased amount of CLDN1 protein in the intestine of $Cdh1^{loxP/loxP}$ Villin-Cre cKO animals compared with controls. In contrast, CLDN4 protein abundance was increased in E-cadherin cKO intestine compared with controls. Although gene array and qRT-PCR data showed Cldn3 to be higher in cKOs compared with controls, immunoblotting did not show a consistent increase in CLDN3 protein in E-cadherin cKO small intestine at E18.5. GAPDH was used as the loading control for these experiments.

cells detached in the lumen suggesting that cell death occurred after detachment from the epithelium.

*Enterocytes are reduced in E-cadherin mutant intestinal epithelium whereas secretory lineages are unchanged*

When dominant-negative N-cadherin was expressed in the villus epithelium, enterocytes were lost (Hermiston and Gordon, 1995a). Moreover, decreased staining for Villin, a marker of the brush border, in small intestine of adult E-cadherin cKO mice also suggested an enterocyte defect in the absence of E-cadherin (Schneider et al., 2010). Based on these data and our gene array data indicating that several metabolic pathways were negatively impacted by loss of E-cadherin in the developing intestinal epithelium (Fig. 3), we examined the status of enterocytes in small intestine of E18.5 E-cadherin cKOs. Array data showed
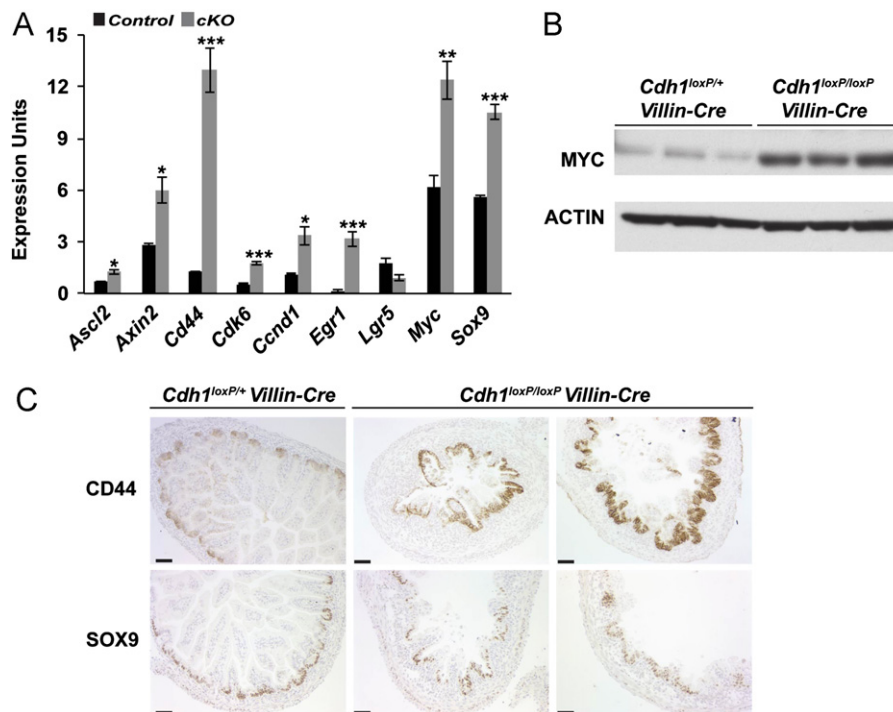
**Fig. 5.** $Cdh1^{loxP/loxP}$ Villin-Cre cKO small intestine contains increased numbers of CD44 and SOX9 positive cells. (A) Cellular proliferation was evaluated using qRT-PCR to compare the abundance of gene products involved in proliferation between the intestinal epithelium of E18.5 control ($n=3$) and $Cdh1^{loxP/loxP}$ Villin-Cre cKOs ($n=3$). All transcripts assayed, except $Lgr5$, were found to be more abundant in cKOs compared with controls. $Gapdh$ was used for normalization. Error bars show SEM. A two-sample Student t test was used to determine $p$-value: $^*p \leq 0.05$, $^{**}p \leq 0.01$, $^{***}p \leq 0.001$ (B) Immunoblot analysis of E18.5 whole cell extracts demonstrated an increased amount of MYC protein in intestine of $Cdh1^{loxP/loxP}$ Villin-Cre cKO animals compared with controls, which is in agreement with gene array and qRT-PCR data showing $Myc$ transcript to be more abundant in intestine of cKOs compared with controls. ACTIN was used as a loading control. (C) Control and E-cadherin mutant E18.5 small intestinal tissue was stained using antibodies against CD44v6 and SOX9. CD44 (brown membrane staining) was properly localized to the intervillus regions, which is the proliferative compartment of the mouse E18.5 small intestine, in control tissue. In contrast, CD44 staining was detected throughout the mutant small intestine epithelium. In addition, staining was more intense in mutant tissue compared with control tissue. SOX9 (brown nuclear staining) was properly localized to the intervillus regions in control tissue. Mutant tissue, however, contained SOX9 positive cells dispersed throughout the epithelium. Sections were counterstained with hematoxylin. Scale bars=50 μm.

$Fabp1$, $Fapb2$, and $Lct$, three canonical enterocyte markers, as significantly decreased in E-cadherin deficient intestine compared with control intestine (Supplemental Table 2), and qRT-PCR confirmed these results (Fig. 7A). Decreases in enterocyte-specific transcripts in E-cadherin cKO embryos could represent single cells expressing these genes at lower levels or a decrease in the total number of cells expressing these markers. Therefore, we used histochemical staining for brush border intestinal alkaline phosphatase activity to examine the enterocyte population in E18.5 control and E-cadherin mutant intestine. Although control tissue stained robustly for alkaline phosphatase activity, E-cadherin deficient tissue either stained weakly or failed to stain for alkaline phosphatase activity (Fig. 7B). Together, these data support the conclusion that the mature enterocyte population is reduced in E-cadherin mutant intestine compared with control.

We also examined the goblet and enteroendocrine lineages in intestines of control and E-cadherin cKO embryos at E18.5. Because Paneth cells do not arise until after birth, these cells could not be evaluated. Alcian blue histochemical staining identified goblet cells in control and mutant intestine. Goblet cells in mutant tissue often stained less intensely compared with those in control tissue (Fig. 7C). We determined the proportion of goblet cells present in the epithelium of control and mutant intestine by counting both total epithelial cells (HNF4+) and alcian blue positive goblet cells in serial sections. We found no significant difference in the percentage of goblet cells present in mutant epithelium compared with control epithelium (control 5.4%, $n=13$ sections, 3 embryos; mutant 6.2%, $n=12$ sections, 3 embryos). In agreement with cell counting data, qRT-PCR demonstrated equivalent expression of the goblet cell markers

$Muc1$, $Muc2$, and $Muc4$ in control and mutant epithelial fractions (Fig. 7A). Unexpectedly, we did detect increased levels of $Muc3$ transcript ($+6.3$ fold) in E-cadherin mutant epithelial fractions compared with control fractions (Fig. 7A). $Muc3$, however, is expressed by intestinal epithelial cell types in addition to goblet cells (Ho et al., 2006; Kim and Ho, 2010). Of interest, MUC3 has been implicated as playing a role in epithelial restitution and wound healing suggesting that its increase reflects a response by the epithelium to counteract the dramatic cell loss caused by E-cadherin deletion (Ho et al., 2006). Immunohistochemical staining for the enteroendocrine cell marker Chromogranin A (ChgA) demonstrated this cell population as present in both control and E-cadherin deficient intestinal epithelium (Fig. 7D). Because enteroendocrine cells represent roughly 1% of the intestinal epithelium, it was difficult to determine if there was a change in ChgA+ cell numbers in mutant tissue by counting since we detected so few of these cells per stained section. Therefore, to get a more accurate assessment of the enteroendocrine cell population, we used qRT-PCR to measure the abundance of enteroendocrine cell markers $Ngn3$ and $ChgA$. These markers were detected at slightly lower amounts in mutant epithelium compared with control (1.5 to 2.0 fold reduced) (Fig. 7A).

### Activated β-catenin is decreased in E-cadherin mutant small intestinal epithelium

It has been proposed that E-cadherin sequesters β-catenin at the cell membrane thereby regulating the pool of nuclear β-catenin available to be transcriptionally active (Van Roy and Berx, 2008). If this is true in the intestinal epithelium, one would
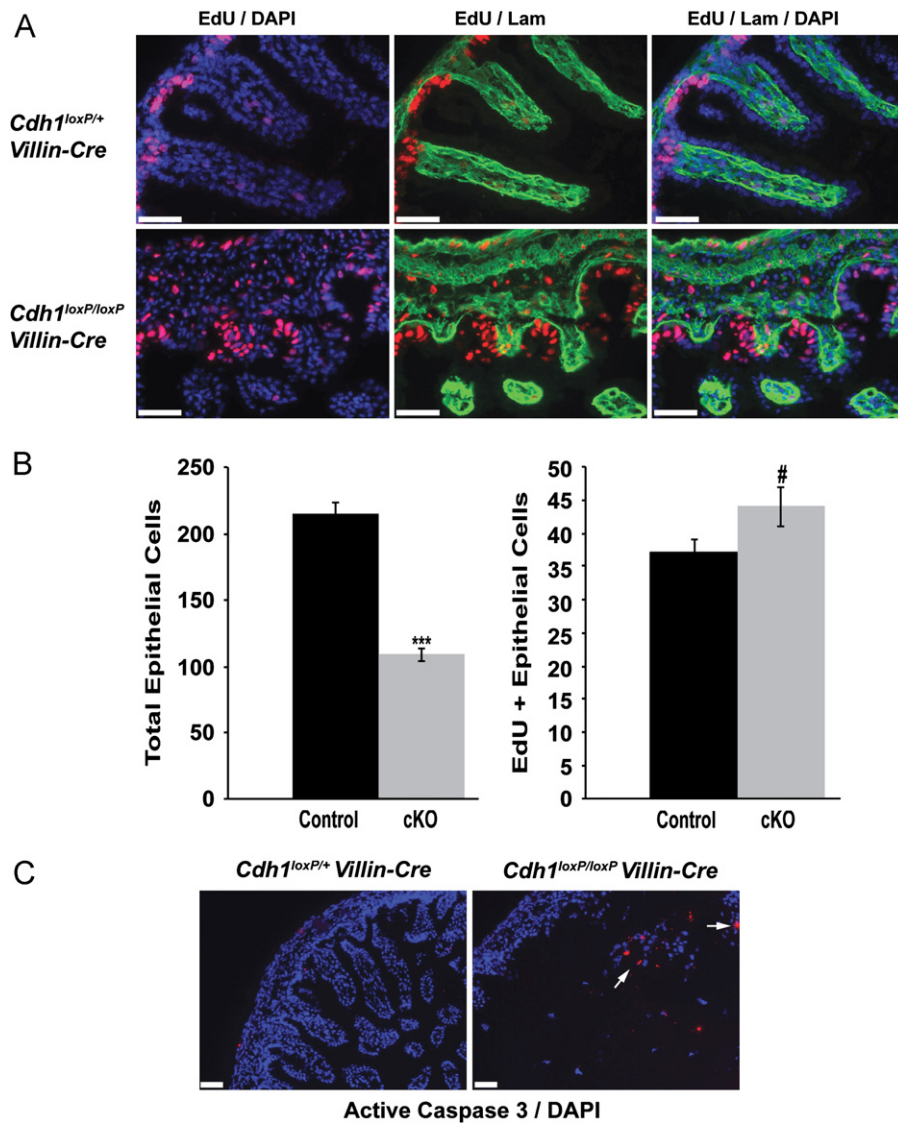
**Fig. 6.** *Cdh1loxP/loxP Villin-Cre* cKO small intestine contains increased proliferative cells compared with control tissue. (A) Proliferation was measured in E18.5 control and *E-cadherin* cKO small intestinal epithelia by staining for EdU incorporation. Because of the severe disruption observed in the mutant tissue, it was difficult to discern proliferating epithelial cells from proliferating mesenchymal cells. Therefore, sections were co-stained using an antibody against a component of the mesenchyme, laminin (left panels, EdU=red, DAPI=blue; center panels, EdU=red, laminin=green; right panels, EdU=red, laminin=green, DAPI=blue). Scale bars=50 μm. (B) Using micrographs of intestinal tissue stained with EdU, Laminin, and DAPI, we counted the total number of epithelial cells (DAPI+, Laminin -) and the number of proliferating epithelial cells (DAPI+, Laminin -, EdU+) in both controls (*n*=9 E18.5 intestines, 53 fields) and mutants (*n*=6 E18.5 intestines, 62 fields). Although the number of total epithelial cells was lower in mutants compared with controls, the number of proliferating epithelial cells was greater in *E-cadherin* cKO small intestine compared with control small intestine (black bars, controls; gray bars, mutants). Error bars show SEM. A two-sample Student t test was used to determine *p*-value (***$p < 0.0001$, #$p=0.0542$). (C) Sections from eight control animals and seven mutant animals were stained with an antibody against active caspase-3 (red staining). DAPI was used to visualize nuclei (blue staining). No change in the number of apoptotic cells associated with the epithelium was detected between *E-cadherin* cKOs and controls. There were, however, increased numbers of sloughed cells in the lumen of mutant tissue staining positive for active caspase-3. Scale bars=50 μm.

predict that deletion of E-cadherin from the intestinal epithelium would result in changes in β-catenin protein distribution in mutant tissue. Moreover, our observation of an increased proliferative population in mutants compared with controls suggests increased β-catenin activity in mutant tissue. Comparison of the abundance of seven β-catenin target transcripts between control and E-cadherin deficient intestinal epithelium – *Ascl2, Axin2, Cd44, Ccnd1, Lgr5, Myc,* and *Sox9* – demonstrated all except *Lgr5* to be increased in E-cadherin mutant epithelium compared with control epithelium (Fig. 5A) (Wnt homepage, http://www.stanford.edu/group/nusselab/cgi-bin/wnt/main and Jubb et al., 2006; Van Der Flier et al., 2009) indicating that activated β-catenin was

indeed increased in mutant epithelium compared with control. Therefore, we collected epithelial cell fractions and analyzed the abundance of β-*catenin* transcript and nuclear activated β-catenin (ABC) protein present in control and mutant intestinal epithelium. An antibody recognizing the active form of β-catenin protein, namely β-catenin dephosphorylated on Ser37 and Thr41 residues, was used in immunoblotting (Staal et al., 2002). To control for the number of epithelial cell nuclei represented in the extracts, we normalized to the level of HNF4a protein, which is a nuclear-localized, epithelial-specific transcription factor. Contrary to our expectation and although there was no change in the level of β-*catenin* mRNA (Fig. 8A), we detected significantly
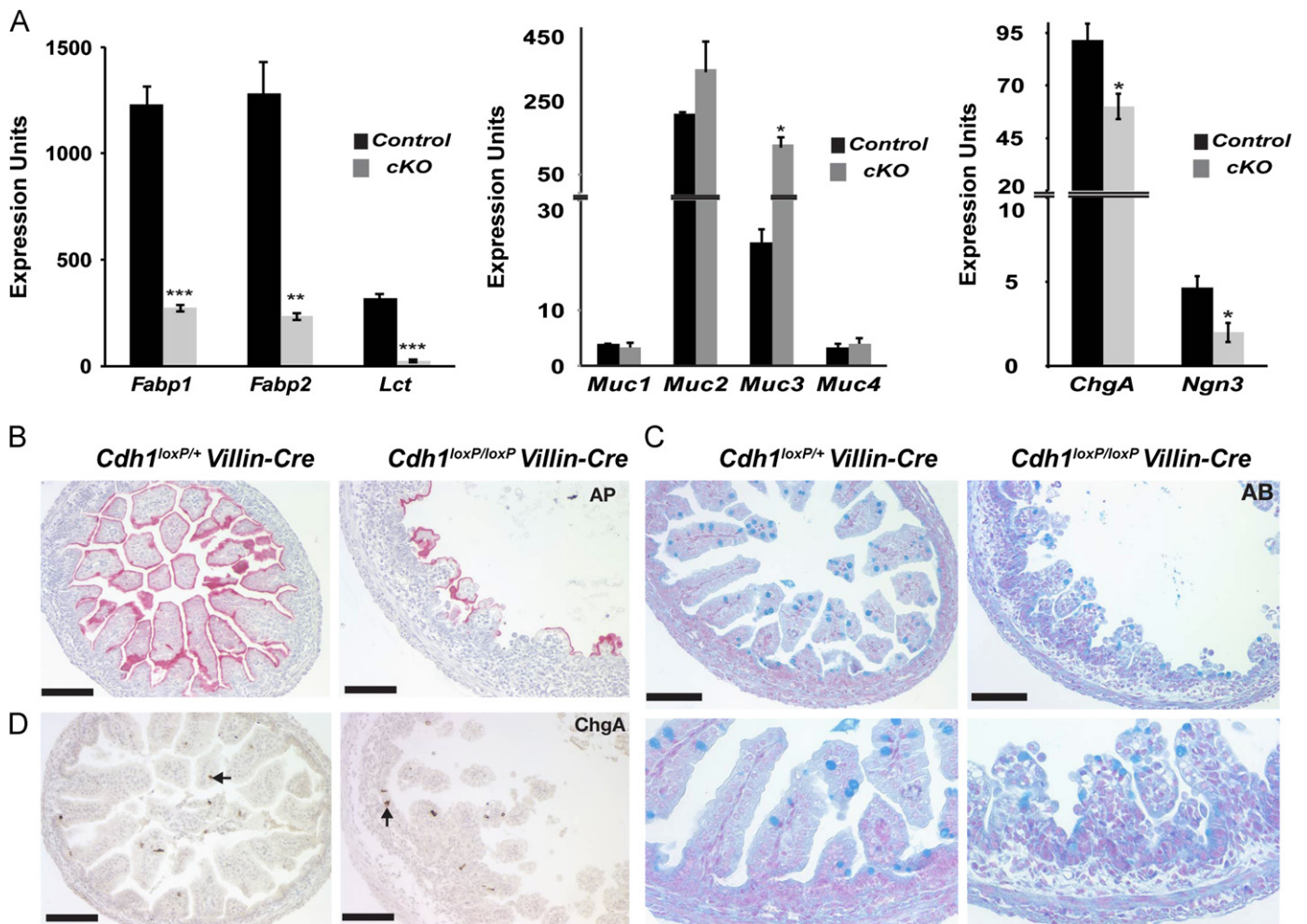
**Fig. 7.** Enterocytes are reduced in E-cadherin deficient small intestinal epithelium. (A) The abundance of markers of specific epithelial cell populations (enterocytes, goblet cells, and enteroendocrine cells) present in the intestinal epithelium of E18.5 control ($n=3$) and $Cdh1^{loxP/loxP}$ Villin-Cre cKOs ($n=3$) was evaluated using qRT-PCR. Markers of the enterocyte population (Fabp1, Fabp2, Lct) were severely decreased in the intestinal epithelium of E-cadherin cKOs compared with controls ($-4.8$, $-5.5$, $-13.0$ fold, respectively). Markers of the goblet cell population (Muc1, Muc2, Muc3, Muc4) were largely unchanged except for a significant increase in Muc3 abundance ($+6.0$ fold). Markers of the enteroendocrine population (ChgA, Ngn3) were slightly lower in the intestinal epithelium of E-cadherin cKOs compared with controls. Gapdh was used for normalization. Error bars show SEM. A two-sample Student t test was used to determine p-value: $^*p \leq 0.05$, $^{**}p \leq 0.01$, $^{***}p \leq 0.001$ (B) Control and E-cadherin mutant E18.5 small intestinal tissue was stained for alkaline phosphatase (AP) activity, a marker of the enterocyte brush border. Alkaline phosphatase activity was robustly detected along the surface of the villi in control tissue (red membrane staining). Although present, alkaline phosphatase positive cells were less abundant in mutant tissue, and the staining intensity was less robust. (C) Control and E-cadherin mutant E18.5 small intestinal tissue was stained with alcian blue (AB) to identify goblet cells. Both control and mutant tissue contained comparable numbers of goblet cells although the intensity of the stain was lesser in some goblet cells present in mutant tissue. Lower panels of C show higher magnification of a region of upper panels. (D) Control and E-cadherin mutant E18.5 small intestinal tissue was stained with an antibody against Chromogranin A (ChgA), a marker of the enteroendocrine population. Both control and mutant tissue contained ChgA+ cells. Sections in all panels were counterstained with hematoxylin. Scale bars = 100 μm.

less activated β-catenin protein in nuclear extracts from E-cadherin mutant intestine compared with control tissue (Fig. 8B and D). In agreement, immunoblotting with an antibody recognizing total β-catenin protein demonstrated lower amounts of total β-catenin protein in nuclear extracts from mutants compared with controls (Fig. 8C and D). Moreover, immunoblotting of cytoplasmic fractions showed decreased amounts of both activated and total β-catenin protein in mutants compared with controls (Fig. 8B, C, and D). Therefore, we conclude that the absence of E-cadherin failed to increase nuclear pools of β-catenin protein. Rather, loss of E-cadherin resulted in decreased amounts of both nuclear and cytoplasmic β-catenin protein. These data suggest that E-cadherin stabilizes cellular β-catenin pools, and in its absence, β-catenin protein is subjected to increased proteolytic degradation.

## Discussion

Taken together, our data uncover a novel and essential role for E-cadherin during embryonic development of the small intestine. Mice lacking E-cadherin specifically in the small intestinal epithelium die shortly after birth. Absence of normal villi and loss of enterocytes in the intestine of E-cadherin mutants suggest decreased surface area for nutrient absorption. Therefore, mutant pups likely died from hypoglycemia because of an absorption defect. Consistent with malnutrition, we detected a trend toward lower serum glucose levels in mutant pups compared with control pups at 5–6 h after birth (Supplemental Fig. 1). It is also possible that decreased feeding contributes to the observed neonatal demise. The presence of a smaller milk spot in mutant pups (Fig. 1A) suggests less feeding by the mutant neonates.
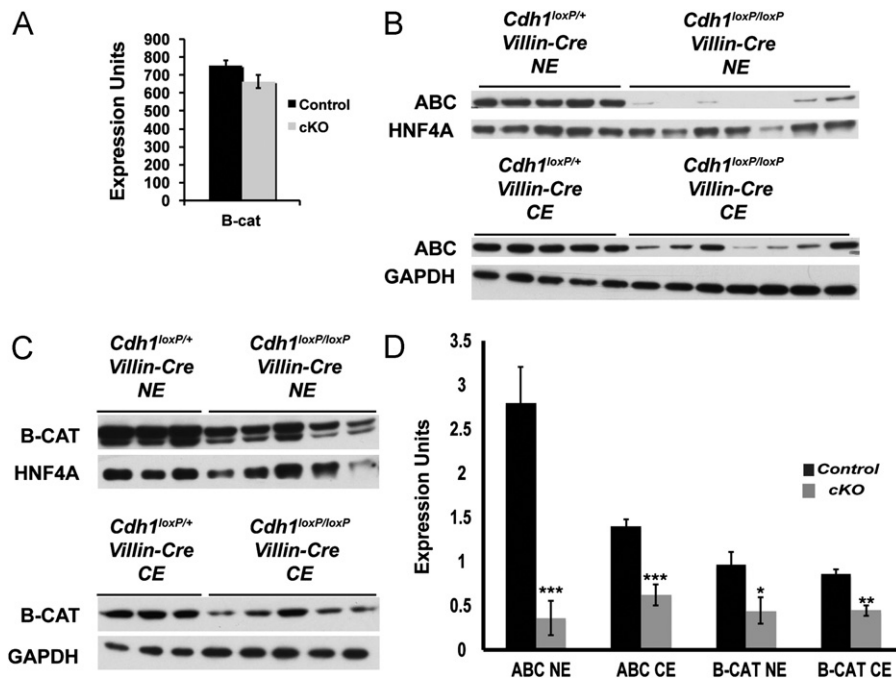
**Fig. 8.** Activated, nuclear-localized β-catenin protein is decreased in *Cdh1^{loxP/loxP} Villin-Cre* cKO intestinal epithelium compared with control epithelium. (A) qRT-PCR demonstrated no change in the abundance of *β-catenin* transcript in the intestinal epithelium of *Cdh1^{loxP/loxP} Villin-Cre* cKOs compared with controls. qRT-PCR was performed using cDNA generated from three independent control and *Cdh1^{loxP/loxP} Villin-Cre* cKO epithelial preparations. *Gapdh* was used for normalization. Error bars show SEM. (B) Immunoblot analysis of E18.5 nuclear (NE) and cytosolic (CE) extracts prepared from epithelial cell fractions of control and E-cadherin mutant intestines was performed using an antibody that recognizes the active form of β-catenin protein, namely β-catenin dephosphorylated at residues Ser37 and Thr41. Such analysis demonstrated a decreased amount of Activated β-catenin (ABC) protein in the intestinal epithelium of *Cdh1^{loxP/loxP} Villin-Cre* cKO animals compared with controls in both fraction types. HNF4a, a nuclear and epithelial specific marker, was used as the loading control for nuclear extracts; GAPDH was used as the loading control for cytosolic extracts. (C) Immunoblot analysis of E18.5 nuclear (NE) and cytosolic (CE) extracts prepared from epithelial cell fractions of control and *E-cadherin* cKO intestines was performed using an antibody that recognizes total β-catenin protein. Such analysis demonstrated a decreased amount of β-catenin (B-CAT) protein in the intestinal epithelium of *Cdh1^{loxP/loxP} Villin-Cre* cKO animals compared with controls in both fraction types. HNF4a (NE) and GAPDH (CE) were used as the loading controls. (D) Blots shown in panels B and C were quantified using densitometry. Graph shows the average abundance of Activated β-catenin (ABC) and total β-catenin (B-CAT) protein present in nuclear (NE) and cytosolic (CE) extracts prepared from epithelial cell fractions of control (black bars) and *E-cadherin* cKO (gray bars) intestines. Control ABC NE and CE $n=5$, cKO ABC NE and CE $n=7$, Control B-CAT NE and CE $n=3$, and cKO B-CAT NE and CE $n=5$. HNF4A (NE) and GAPDH (CE) were used for normalization. Error bars show SEM. A two-sample Student t test was used to determine *p*-value: $*p=0.05931$, $**p \leq 0.01$, $***p \leq 0.001$.

In contrast to Schneider et al. (2010), who observed loss of desmosomes in a model of E-cadherin deletion in the adult mouse intestinal epithelium, we identified junctional complexes containing desmosomes in E-cadherin deficient embryonic intestinal epithelium (Fig. 2). Our data, however, demonstrated that although junctional complexes were present in the intestinal epithelium of *E-cadherin* cKO E18.5 embryos, these junctions were abnormal, appearing abbreviated in mutants. Moreover, the junctions present in mutant tissue failed to block paracellular transport of small tracer molecules demonstrating defective barrier function in the absence of E-cadherin. This agrees with the findings of Tunggal et al. (2005) who showed a barrier defect in epidermis lacking E-cadherin. Our findings together with those of Schneider et al. (2010) suggest that the role of E-cadherin in junctional complex assembly and maintenance differs depending upon the maturity of the intestinal epithelium.

Selectivity and strength of tight junctions in a given tissue is thought to be regulated by the combination of claudin proteins composing tight junctions (Schneeberger and Lynch, 2004; Hewitt et al., 2006). Our observation that CLDN1 and CLDN4 protein levels were dramatically altered in E-cadherin deficient epithelium provides an explanation for the increased tight junction permeability present in mutant epithelium. Analysis of animals lacking *Cldn1* in the skin demonstrated a crucial role for this claudin protein in epidermal tight junction function. Neonates lacking epidermal *Cldn1* died because of water loss (Furuse et al., 2002). Moreover, mice lacking E-cadherin in the epidermis had decreased amounts of CLDN1 protein in the skin, and these neonates also died because of water barrier failure (Tunggal et al., 2005). CLDN4 protein was also decreased in E-cadherin deficient skin (Tunggal et al., 2005). Deletion of E-cadherin in the intestine in our system, however, led to increased CLDN4 protein in E-cadherin mutants compared with controls. CLDN4 was virtually absent from control intestine but was highly abundant in E-cadherin mutant intestine. These data suggest that although E-cadherin plays a role in regulating tight junction permeability through claudin proteins, the exact mechanism through which this occurs varies among organs.

We report increased proliferation in E-cadherin deficient intestinal epithelium compared with control epithelium. Similar changes in proliferation were observed in other studies of E-cadherin in the small intestine. Expression of dominant-negative N-cadherin (NCADΔ) in the intestinal epithelium led to an expansion of the proliferative zone in the crypt, whereas over-expression of E-cadherin in the intestinal epithelium resulted in decreased proliferation (Hermiston and Gordon, 1995a; Hermiston et al., 1996). Moreover, conditional knockout of E-cadherin in the adult small intestine resulted in a markedly expanded proliferative zone (Schneider et al., 2010). We conclude that the increased number of proliferative cells observed in *E-cadherin* cKO mice likely occurred as a compensatory response to repair the severely disrupted architecture of the intestinal epithelium. Hermiston and Gordon (1995a) drew a similar conclusion regarding increased proliferation observed in intestinal crypts of mice expressing NCADΔ protein. Because E-cadherin deficient intestinal epithelium contained fewer total epithelial cells compared with control epithelium, we conclude that increasing the number of proliferative cells was not sufficient to rescue epithelial cell numbers.

Examination of the differentiated intestinal epithelial cell populations present in *E-cadherin* cKOs demonstrated a reduced number of enterocytes compared with controls. The simplest explanation of this observation is that E-cadherin deletion disrupts cell adhesion thereby allowing enterocytes localized on the villi to slough into the lumen. Electron microscopy revealed large gaps between epithelial cells in *E-cadherin* cKO intestinal tissue, whereas control epithelial cells were tightly juxtaposed with each other. Moreover, we frequently observed cellular debris in the lumen of gut. Other studies of E-cadherin deficient organs, however, demonstrated defective differentiation in the absence of E-cadherin. Boussadia et al. (2002) showed that loss of E-cadherin in the mammary gland impaired terminal differentiation of the alveolar epithelium of the lactating mammary gland. Moreover, Young et al. (2003) demonstrated that E-cadherin is required for proper differentiation of keratinocytes. Therefore, our observation of an increased number of proliferative cells in small intestine lacking E-cadherin compared with controls may reflect a shift from differentiation toward proliferation. Increased proliferation, however, could also occur as a compensatory response to combat loss of enterocytes as discussed above. Our data cannot discriminate between these two scenarios.

If our observation of increased proliferative cells and decreased enterocytes reflects a shift from differentiation to proliferation, we would expect to see similar loss of other differentiated epithelial cell types, namely goblet cells and enteroendocrine cells. We found that the proportion of goblet cells present in *E-cadherin* cKO tissue as well as the expression of goblet cell markers were virtually unchanged in mutants compared with controls suggesting that the observed reduction of the enterocyte population cannot be completely explained by loss of cells because of cell adhesion defects. Although we were not able to count reliably the number of enteroendocrine cells given these cells are rare, measurement of enteroendocrine cell transcripts revealed only subtle decreases in these markers (less than 2 fold changes) suggesting that this population was subtly impacted if at all. Based on these findings, we cannot exclude the possibility that in addition to cell loss because of compromised cell adhesion, E-cadherin deletion selectively disrupts the enterocyte differentiation program in *E-cadherin* cKOs.

Because we observed an increase in the proliferative cell population and a concomitant increase in multiple β-catenin target gene mRNAs, we expected to detect increased accumulation of nuclear active β-catenin protein in E-cadherin mutants compared with controls. We found, however, a 7.7 fold decrease in the amount of nuclear activated β-catenin protein present in E-cadherin mutant epithelium compared with control epithelium. The level of cytosolic activated β-catenin protein as well as that of total β-catenin protein present in E-cadherin deficient epithelium was also lower compared with control tissue. Similar to our results, elimination of E-cadherin from the epidermis as well as the thyroid resulted in decreased abundance of β-catenin protein (Tinkle et al., 2004; Tunggal et al., 2005; Cali et al., 2007). One explanation for our paradoxical β-catenin finding, namely that β-catenin target gene mRNAs increased in abundance while β-catenin protein itself decreased, is that β-catenin target gene expression occurred as a result of a β-catenin-independent transcriptional pathway in mutant epithelium. One such pathway is mediated through a closely related catenin family member, junction plakoglobin (γ-catenin), which has been shown to respond to Wnt ligands to both positively and negatively influence gene transcription (McCrea et al., 2009). Moreover, junction plakoglobin has been shown to activate TCF/LEF-dependent transcription in β-catenin deficient cell lines (Maeda et al., 2004; Kim et al., 2011). It is also possible that antagonists of β-catenin transactivation are expressed at lower levels in mutant epithelium thereby effectively lowering the threshold of nuclear β-catenin required to activate transcription. Our oligonucleotide array data uncovered two molecules related to known β-catenin antagonists as less abundant in

mutant tissue compared with control tissue. *Dapper homolog 2, antagonist of beta-catenin* (*xenopus*) (*Dact2*) and *Disabled-1* (*Dab1*) were decreased -2.0 and -3.9 fold, respectively. Although these molecules have not yet been shown to modulate β-catenin activity, their related family members DACT1 and DAB2 do negatively impact β-catenin transactivation (Gao et al., 2008; Jiang et al., 2009).

## Conclusions

Based on these data, we conclude that intestinal E-cadherin is required for the formation of a functional intestinal epithelium in mice. Without E-cadherin in the intestine, animals fail to survive. Our studies highlight a key role for E-cadherin in intestinal epithelial morphogenesis and homeostasis during embryonic development. The phenotype observed likely occurs as result of both direct and indirect effects of E-cadherin loss. Breakdown of adherens junctions themselves as well as disruption of the signaling pathways regulated by adherens junctions both may impact intestinal development and, therefore, aspects of the observed phenotype. Moreover, there are likely compensatory events occurring in the face of such a dramatic disruption to epithelial architecture.

## Grant support

## Conflicts of interest

No conflicts of interest exist.

## Transcript profiling

Microarray data from this study have been deposited into NCBI Gene Expression Omnibus (GEO, http://www.ncbi.nlm.nih.gov/geo) and are accessible through GEO series accession number GSE31771.

## Acknowledgments

## Appendix A. Supporting information

Supplementary data associated with this article can be found in the online version at http://dx.doi.org/10.1016/j.ydbio.2012.06.005.

## References

Bancroft, J. D., Gamble, M., 2007. Theory and Practice of Histological Techniques.
Bastide, P., Darido, C., Pannequin, J., Kist, R., Robine, S., Marty-Double, C., Bibeau, F., Scherer, G., Joubert, D., Hollande, F., Blache, P., Jay, P., 2007. Sox9 regulates cell

proliferation and is required for Paneth cell differentiation in the intestinal epithelium. J. Cell Biol. 178, 635–648.

Battle, M.A., Konopka, G., Parviz, F., Gaggl, A.L., Yang, C., Sladek, F.M., Duncan, S.A., 2006. Hepatocyte nuclear factor 4alpha orchestrates expression of cell adhesion proteins during the epithelial transformation of the developing liver. Proc. Nat. Acad. Sci. U.S.A. 103, 8419–8424.

Boussadia, O., Kutsch, S., Hierholzer, A., Delmas, V., Kemler, R., 2002. E-cadherin is a survival factor for the lactating mouse mammary gland. Mech. Dev. 115, 53–62.

Cali, G., Zannini, M., Rubini, P., Tacchetti, C., D'Andrea, B., Affuso, A., Wintermantel, T., Boussadia, O., Terracciano, D., Silberschmidt, D., Amendola, E., De Felice, M., Schutz, G., Kemler, R., Di Lauro, R., Nitsch, L., 2007. Conditional inactivation of the E-cadherin gene in thyroid follicular cells affects gland development but does not impair junction formation. Endocrinology 148, 2737–2746.

Cavallaro, U., Dejana, E., 2011. Adhesion molecule signalling: not always a sticky business. Nat. Rev. Mol. Cell. Biol. 12, 189–197.

Furuse, M., Hata, M., Furuse, K., Yoshida, Y., Haratake, A., Sugitani, Y., Noda, T., Kubo, A., Tsukita, S., 2002. Claudin-based tight junctions are crucial for the mammalian epidermal barrier: a lesson from claudin-1-deficient mice. J. Cell Biol. 156, 1099–1111.

Gao, X., Wen, J., Zhang, L., Li, X., Ning, Y., Meng, A., Chen, Y., 2008. Dapper1 is a nucleocytoplasmic shuttling protein that negatively modulates Wnt signaling in the nucleus. J. Biol. Chem. 283, 35679–35688.

Gumbiner, B., Stevenson, B., Grimaldi, A., 1988. The role of the cell adhesion molecule uvomorulin in the formation and maintenance of the epithelial junctional complex. J. Cell Biol. 107, 1575–1587.

Hermiston, M., Gordon, J., 1995a. In vivo analysis of cadherin function in the mouse intestinal epithelium: essential roles in adhesion, maintenance of differentiation, and regulation of programmed cell death. J. Cell Biol. 129, 489–506.

Hermiston, M., Gordon, J., 1995b. Inflammatory bowel disease and adenomas in mice expressing a dominant negative N-cadherin. Science 270, 1203–1207.

Hermiston, M., Wong, M., Gordon, J., 1996. Forced expression of E-cadherin in the mouse intestinal epithelium slows cell migration and provides evidence for nonautonomous regulation of cell fate in a self-renewing system. Genes Dev. 10, 985–996.

Hewitt, K., Agarwal, R., Morin, P., 2006. The claudin gene family: expression in normal and neoplastic tissues. BMC Cancer 6, 186.

Ho, S., Dvorak, L., Moor, R., Jacobson, A., Frey, M., Corredor, J., Polk, D., Shekels, L.L., 2006. Cysteine-rich domains of muc3 intestinal mucin promote cell migration, inhibit apoptosis, and accelerate wound healing. Gastroenterology 131, 1501–1517.

Jiang, Y., Luo, W., Howe, P., 2009. Dab2 stabilizes Axin and attenuates Wnt/beta-catenin signaling by preventing protein phosphatase 1 (PP1)-Axin interactions. Oncogene 28, 2999–3007.

Jubb, A., Chalasani, S., Frantz, G.D., Smits, R., Grabsch, H.I., Kavi, V., Maughan, N.J., Hillan, K.J., Quirke, P., Koeppen, H., 2006. Achaete-scute like 2 (ascl2) is a target of Wnt signalling and is upregulated in intestinal neoplasia. Oncogene 25, 3445–3457.

Kim, Y., Ma, H., Oehler, V., Gang, E., Nguyen, C., Masiello, D., Liu, H., Zhao, Y., Radich, J., Kahn, M., 2011. The gamma catenin/CBP complex maintains survivin transcription in beta-catenin deficient/depleted cancer cells. Curr. Cancer Drugs Targets 11, 213–225.

Kim, Y., Ho, S.B., 2010. Intestinal goblet cells and mucins in health and disease: recent insights and progress. Curr. Gastroenterol. Rep. 12, 319–330.

Larue, L., Ohsugi, M., Hirchenhain, J., Kemler, R., 1994. E-cadherin null mutant embryos fail to form a trophectoderm epithelium. Proc. Nat. Acad. Sci. U.S.A. 91, 8263–8267.

Lewis, P.R., Knight, D., 1992. Cytochemical staining methods for electron microscopy. Pract. Methods Electron Microsc. 14, 174–178.

Li, C., Wong, W.H., 2001. Model-based analysis of oligonucleotide arrays: expression index computation and outlier detection. Proc. Nat. Acad. Sci. U.S.A. 98, 31–36.

Li, X., Madison, B., Zacharias, W., Kolterud, A., States, D., Gumucio, D., 2007. Deconvoluting the intestine: molecular evidence for a major role of the mesenchyme in the modulation of signaling cross talk. Physiol Genomics 29, 290–301.

Madison, B.B., Dunbar, L., Qiao, X.T., Braunstein, K., Braunstein, E., Gumucio, D.L., 2002. Cis elements of the villin gene control expression in restricted domains of the vertical (crypt) and horizontal (duodenum, cecum) axes of the intestine. J. Biol. Chem. 277, 33275–33283.

Madison, B., Braunstein, K., Kuizon, E., Portman, K., Qiao, X., Gumucio, D., 2005. Epithelial hedgehog signals pattern the intestinal crypt-villus axis. Development 132, 279–289.

Maeda, O., Usami, N., Kondo, M., Takahashi, M., Goto, H., Shimokata, K., Kusugami, K., Sekido, Y., 2004. Plakoglobin (gamma-catenin) has TCF/LEF family-dependent transcriptional activity in beta-catenin-deficient cell line. Oncogene 23, 964–972.

McCrea, P.D., Gu, D., Balda, M., 2009. Junctional music that the nucleus hears: cell-cell contact signaling and the modulation of gene activity. Cold Spring Harb Perspect. Biol. 1, a002923.

Perez-Moreno, M., Jamora, C., Fuchs, E., 2003. Sticky business: orchestrating cellular signals at adherens junctions. Cell 112, 535–548.

Schneeberger, E.E., Lynch, R.D., 2004. The tight junction: a multifunctional complex. Am. J. Physiol. Cell. Physiol. 286, C1213–C1228.

Schneider, M., Dahlhoff, M., Horst, D., Hirschi, B., Trulzsch, K., Muller-Hocker, J., Vogelmann, R., Allgauer, M., Gerhard, M., Steininger, S., Wolf, E., Kolligs, F., 2010. A key role for E-cadherin in intestinal homeostasis and Paneth cell maturation. PLoS One 5, e14325.

Sherr, C., 1995. D-type cyclins. Trends Biochem. Sci. 20, 187–190.

Spence, J., Lauf, R., Shroyer, N., 2011. Vertebrate intestinal endoderm development. Dev. Dyn. 240, 501–520.

Staal, F., Noort, Mv, M., Strous, G., Clevers, H., 2002. Wnt signals are transmitted through N-terminally dephosphorylated beta-catenin. EMBO Rep. 3, 63–68.

Tinkle, C.L., Lechler, T., Pasolli, H.A., Fuchs, E., 2004. Conditional targeting of E-cadherin in skin: insights into hyperproliferative and degenerative responses. Proc. Nat. Acad. Sci. U.S.A. 101, 552–557.

Troxell, M.L., Gopalakrishnan, S., Mccormack, J., Poteat, B., Pennington, J., Garringer, S., Schneeberger, E., Nelson, W., Marrs, J., 2000. Inhibiting cadherin function by dominant mutant E-cadherin expression increases the extent of tight junction assembly. J. Cell Sci. 113, 985–996.

Tunggal, J.A., Helfrich, I., Schmitz, A., Schwarz, H., Gunzel, D., Fromm, M., Kemler, R., Krieg, T., Niessen, C.M., 2005. E-cadherin is essential for in vivo epidermal barrier function by regulating tight junctions. EMBO J. 24, 1146–1156.

Van Der Flier, L.G., Van Gijn, M.E., Hatzis, P., Kujala, P., Haegebarth, A., Stange, D., Begthel, H., Van Den Born, M., Guryev, V., Oving, I., Van Es, J.H., Barker, N., Peters, P., Van De Wetering, M., Clevers, H., 2009. Transcription factor achaete scute-like 2 controls intestinal stem cell fate. Cell 136, 903–912.

Van Roy, F., Berx, G., 2008. The cell-cell adhesion molecule E-cadherin. Cell. Mol. Life Sci. 65, 3756–3788.

Young, P., Boussadia, O., Halfter, H., Grose, R., Berger, P., Leone, D.P., Robenek, H., Charnay, P., Kemler, R., Suter, U., 2003. E-cadherin controls adherens junctions in the epidermis and the renewal of hair follicles. EMBO J. 22, 5723–5733.